On the Measurement of Positive Soret Coefficients

J. F. Dutrieux,[†] J. K. Platten,[*,†] G. Chavepeyer,[†] and M. M. Bou-Ali[‡]

General Chemistry Service, University of Mons-Hainaut, Mons, Avenue du Champs de Mars, 24, Belgium and Departamento de Ingenieria Mecanica Energetica y de Materiales, Universidad Publica de Navarra, Pamplona, Spain

Received: October 25, 2001; In Final Form: February 25, 2002

In this paper, we report Soret coefficients obtained by two independent methods and for two different systems-(water-ethanol containing respectively 60.88 and 50 wt % of water). The Soret coefficient is defined by $S_T = D_T/D$ where D_T is the thermal diffusion coefficient, and D is the isothermal diffusion coefficient. In the first method, D_T is determined by a 5-point sampling process in a thermogravitational column and D by the well-known OEC technique (open-ended capillary). The ratio of the experimental values of D_T and D gives the expected value of S_T. A totally new method consists of velocity measurements of a transient natural convective state: indeed, the Soret effect induces modifications of density gradients and therefore of the buoyancy responsible for free or natural convection. The modifications of the convective amplitudes are thus an indirect way to have access to the Soret coefficient. The velocity measurements were obtained by LDV. The comparison between the two techniques shows a deviation of the order of 4%, which is quite satisfactory. The agreement with the literature is also excellent.

1. Introduction

In a binary mixture, initially homogeneous, submitted to a temperature gradient, the Soret effect induces a concentration (or mass fraction) gradient

$$\mathrm{grad}c = -\frac{D_T}{D}c_0(1-c_0)\mathrm{grad}T \qquad (1)$$

In eq 1, D_T is the thermal diffusion coefficient, D is the ordinary (isothermal) diffusion coefficient, and c_0 is the initial value of the mass fraction c of the component to which D_T is referred. The ratio D_T/D is called the Soret coefficient S_T. In the remainder of this paper, the component specified by its mass fraction c will be taken (arbitrarily) to be the denser. Of course, the opposite convention could be adopted. Thus, when $S_T = D_T/D > 0$, grad$c$ is of opposite sign to grad$T$. In other words, c decreases approaching the hot wall of the container: the denser component migrates to the cold wall, and the lighter to the hot wall. The accurate measurement of S_T still remains a challenge for two reasons. First, owing to the small value of S_T (generally of the order of 10^{-3} K^{-1}), the resulting mass fraction gradient remains small, usually less than 1% mass fraction difference between the two walls. Moreover, eq 1 is only valid in a convection-free experiment; in other words, when the temperature gradient is parallel to the gravity field and smaller than some critical value to avoid instability. This is the pure Soret configuration (a horizontal liquid layer heated from above). But even in that case, some people believe that it is difficult to avoid any convective perturbation linked, for example, to a small tilt angle with respect to the perfect horizontal direction, or to small horizontal gradients due to a bad lateral insulation of the experimental cell or some other reason.[1,2] Therefore, microgravity experiments have been proposed and performed.[2] It is not clear today if routine experiments may or may not be performed in microgravity, due to the limited number of flights. This situation could change in the future when the International Space Station (ISS) will be fully operational. It is our opinion today that alternative ways for measuring S_T should be investigated. Instead of trying to avoid convection, we have used an alternative approach: convective coupling in vertical thermogravitational columns (TGC), a technique described for the first time in 1939 by Clusius and Dickel.[3] The liquid is enclosed in a vertical slot of large aspect ratio (Figure 1) $Lz \gg Lx$ (typically $Lz/Lx > 100$), the two vertical walls being maintained at two different temperatures T_{hot} and T_{cold}. When $S_T > 0$, the lighter (denser) component migrates to the hot (cold) wall and by convection is advected to the top (bottom) of the cell, creating a vertical mass fraction gradient not predicted by eq 1, due to the coupling with convection. This process has received a great deal of attention mainly due to possible industrial separation (e.g., of isotopes). One could also mention that the coupling between the Soret effect (induced by the geothermal gradient) and convection could be important to predict the present state of oil reservoirs.[4] In this case, the theory should be extended to multicomponent mixtures. But, as a matter of fact, we first must be able to accurately measure Soret coefficients in binary mixtures, before proceeding with ternary and then polynary mixtures. The aim of this paper is to propose two independent techniques (an "old" one, modified to improve accuracy, and a totally new one) in the same experimental cell. The "old" technique relies on the vertical mass fraction gradient, as studied analytically by several authors[5−8] and more recently numerically,[9] in order to validate the analytical treatment in which some unavoidable simplifying assumptions were made. It has been shown in all of those papers that, when the spacing Lx is "large

* To whom correspondence should be addressed. E-Mail: jean.platten@umh.ac.be.

[†] General Chemistry Service, University of Mons-Hainaut. Fax: +32-65373510. E-mail: jean-francois.dutrieux@umh.ac.be, guy.chavepeyer@umh.ac.be.

[‡] Departamento de Ingenieria Mecanica Energetica y de Materiales, Universidad Publica de Navarra. E-mail: mounir.bouali@upna.es.

10.1021/jp013945r CCC: $22.00
Published on Web 05/17/2002

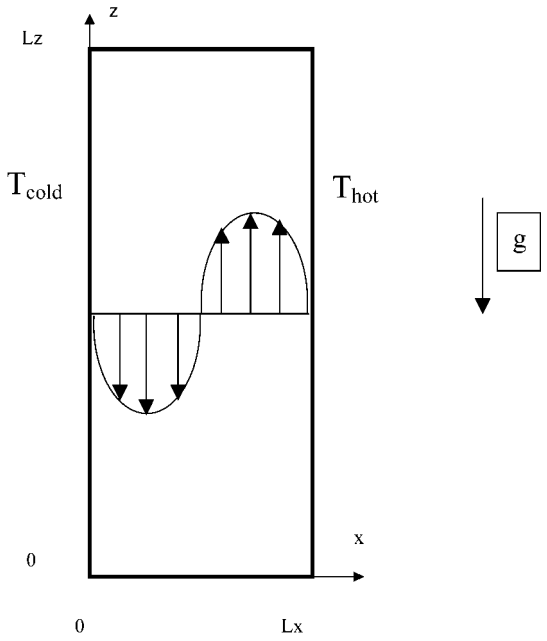

Figure 1. Sketch of the 2D thermogravitational column.

enough", say larger than 1 mm (but this value depends on the physical parameters of the liquid, including its viscosity, thermal expansion coefficient, isothermal diffusion coefficient...), then the vertical mass fraction gradient (or more precisely the difference in mass fraction between bottom and top Δc) is approximately given by

$$\Delta c \cong 504 \frac{\nu}{\alpha g} D_T c_0 (1 - c_0) \frac{Lz}{Lx^4} \tag{2}$$

where ν is the kinematic viscosity, α the thermal expansion coefficient, and g the gravity acceleration. In the simplified eq 2, the difference of temperature ΔT between the two vertical walls is absent and this fact is justified later in the section 2.2. Many experiments performed recently are based on eq 2[10−12] but the procedure has been used for a long time already.[13] Unfortunately in all these previous experiments, the value of Δc is based on a ≪ two-point ≫ measurement, and could result in a loss of accuracy. Moreover, the technique provides D_T, not the Soret coefficient itself. Therefore, the isothermal diffusion coefficient is usually taken from literature when available, or sometimes from the time evolution $\Delta c(t)$ toward its steady value. But such a procedure is time-consuming as explained in.[14] We prefer to measure D in an isothermal experiment. The so-called "open-ended capillary" (OEC) technique[15] seems very simple and precise (estimated error less than 5%). We have developed this technique in our laboratory to determine D, together with the measurement of the vertical mass fraction distribution $c(z)$, based on a five-point sampling process, that finally gives D_T based on eq 2. The estimated accuracy is also better than 5%. Thus, these two separate experiments allow the evaluation of $S_T = D_T/D$.

The new technique is based on the modification of the velocity field under the action of the Soret effect. Indeed, the density of the liquid mixture ρ is not only a function of the local temperature, T, but also of the local mass fraction c. We assume a linear law which is quite reasonable for small temperature and mass fraction differences

$$\rho = \rho_0[1 - \alpha(T - T_0) + \beta(c - c_0)] \tag{3}$$

In eq 3, the index 0 refers to the mean values of the different quantities. α and β are the thermal and mass expansion coefficients defined respectively by

$$\alpha = -\frac{1}{\rho_0}\left(\frac{\partial \rho}{\partial T}\right)_{c=c_0} > 0 \tag{4a}$$

$$\beta = \frac{1}{\rho_0}\left(\frac{\partial \rho}{\partial c}\right)_{T=T_0} > 0 \tag{4b}$$

They are both positive because c is the denser component. The buoyancy force ρg is thus affected by the Soret effect. However, in the steady state, because c is mainly a function of the vertical coordinate with a stable vertical stratification, the contribution of the horizontal mass fraction gradient to buoyancy is usually neglected: this has been termed the "forgotten effect" by De Groot[8] because it has been "forgotten" or neglected in the original paper of Furry et al.[5] But this assumption can only be true in the steady state. In the transient state, the Soret effect acts initially to create a horizontal mass fraction gradient, in the direction of the temperature gradient. Therefore, in the pure "diffusive" regime, well before the establishment of the final steady convective regime with $(\partial c/\partial z) \neq 0$, the mass fraction is only a function of x, with $(\partial c/\partial x)$ given by eq 1. Because the lighter component migrates to the hot plate, its effect is to lower the local density there. Therefore, the horizontal density gradient $(\partial \rho/\partial x)$ will be larger in the pure diffusive regime than in the steady state. The result will be a larger velocity amplitude. As already said, this effect can only be transient in time. In other words, there is a transient overshoot in the velocity amplitude compared to the velocity amplitude in the steady state. This overshoot is related to the Soret effect and, as shown in section 2, gives $S_T = D_T/D$ directly. We have thus measured the vertical velocity amplitudes with time using Laser Doppler Velocimetry (LDV). Let us emphasize that the LDV experiments were performed in strictly the same experimental cell used for the sampling process. We have thus three independent experiments providing two independent values of S_T, and if the two values of S_T agree, we may have confidence in the proposed values.

Two systems were investigated: water−ethanol (60.88 wt % of water) and water-ethanol (50 wt % of water). The first was chosen because it has been studied recently, at least to our knowledge, by four independent groups of researchers[16−19] and therefore is a prime candidate to test any new technique. The second system have never been investigated before, but was selected because we suspected a higher value of S_T, resulting in a more pronounced Soret contribution to density gradients. In all of our experiments, the mean temperature was kept constant $T_0 = 22.5$ °C ($T_{hot} = 25$ °C and $T_{cold} = 20$ °C).

This paper is organized as follows: In section 2, we give the necessary theoretical support (working equations to deduce D_T, D, and S_T). In section 3, the results concerning the measurement of D by the OEC technique are provided. In section 4, we describe the thermogravitational column (TGC) together with the five-point sampling process and the deduced value of D_T. In section 5, the LDV experiments are given. A comparison between the different techniques and results from other laboratories and conclusions are given in section 6.

2. Theory or Working Equations. *2.1. Theory of the OEC Technique.* We briefly recall here the main features of the OEC technique to measure D.[15] In isothermal conditions a capillary, or better a small tube, with an upper open end is filled with an homogeneous binary solution characterized by an initial mass fraction c_0. This capillary is immersed in an "infinite" bath (i.e., of very large volume compared to that of the tube) of mass

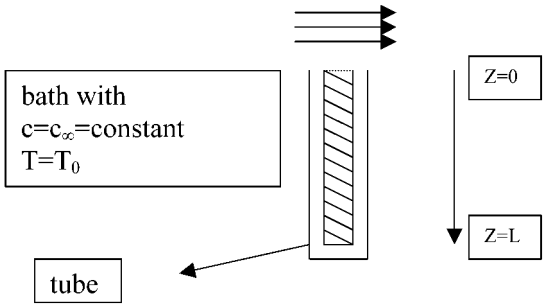

Figure 2. Experimental conditions of the OEC method.

fraction c_∞ and diffusion, described by the one-dimensional Fick's law

$$\frac{\partial c}{\partial t} = D\frac{\partial^2 c}{\partial z^2} \tag{5}$$

continues until equilibrium, i.e., $c = c_\infty$ everywhere, because we suppose the bath to be infinite. Equation 5 is solved with the following initial and boundary conditions (see Figure 2)

$$c(z,t=0) = c_0$$

$$c(z=0,t>0) = c_\infty$$

$$\frac{\partial c}{\partial z} = 0 \text{ at } z = L \tag{6}$$

One should take care of the fact $c_\infty < c_0$ in order to avoid a mass flux outward the tube by natural convection. Also in order to keep the mass fraction always equal to c_∞ at the upper boundary, a very small laminar flow is imposed parallel to the surface (see[15] for more details). The solution of eq 5 with conditions 6 is easily obtained

$$c(z,t) - c_\infty = \frac{4}{\pi}(c_0 - c_\infty)\sum_{n=0}^{\infty}\frac{\sin\left[\left(n+\frac{1}{2}\right)\pi\frac{z}{L}\right]}{2n+1}e^{-(n+1/2)^2(\pi^2/L^2)Dt} \tag{7}$$

and next averaged over the length of the capillary.

Defining

$$\langle c(t)\rangle = \frac{1}{L}\int_0^L c(z,t)dz \tag{8}$$

we get

$$\langle c(t)\rangle - c_\infty = \frac{8(c_0 - c_\infty)}{\pi^2}\sum_{n=0}^{\infty}\frac{e^{-(n+(1/2))^2(\pi^2/L^2)Dt}}{(2n+1)^2} \tag{9}$$

The series 9 converges very quickly and when $\pi^2 Dt/4L^2 \geq 0.05$. The dominant term $n = 0$ is sufficient to provide the necessary working equation

$$\ln\left(\frac{\pi^2(\langle c(t)\rangle - c_\infty)}{8(c_0 - c_\infty)}\right) = -\frac{\pi^2}{4L^2}Dt \tag{10}$$

Thus, the time evolution of $\langle c(t)\rangle$ gives the mean isothermal diffusion coefficient $\bar{D}$, in the range $[c_0, c_\infty]$

$$\bar{D} = \frac{1}{c_0 - c_\infty}\int_{c_\infty}^{c_0} D(c)dc \tag{11}$$

It is therefore preferable to keep c_0 and c_∞ close to each other, so that D may be considered as almost constant in this range. The value of $\bar{D}$ is then supposed to be that of D calculated at a mass fraction $c = (c_0 + c_\infty)/2$.

2.2. Mass Separation in TGC. We recall very quickly the results of the theory of Furry, Jones, and Onsager[5,6] and its extension to concentrated solutions by Majumdar,[7] hereafter called the FJOM theory. Let us quote some simplifying assumptions.

- The aspect ratio $A = Lz/Lx$ of the TGC is very high ($A > 100$).
- Therefore, the horizontal velocity component u is neglected (but this is certainly not true near the upper and the lower boundaries).
- The pure diffusive regime is supposed to describe the temperature field ($T(x)$ is a linear function of x; no vertical temperature gradient).
- The usual Boussinesq approximation.
- The density is only a function of T (already called the forgotten effect).

The molecular separation, i.e., the difference Δc in mass fraction between top and bottom of the TGC is governed by two constants, H and K_t

$$H = \alpha\rho g D_T \Delta T^2 \frac{Lx^3}{(6!\nu D)} \tag{12a}$$

$$K_t = K + K_d = \alpha^2\rho g^2 \Delta T^2 \frac{Lx^7}{(9!\nu^2 D)} + Lx\rho D \tag{12b}$$

Defining $q = e^{(HLz/K_t)}$, the FJOM theory gives Δc

$$\Delta c = (q^{c_0} - 1)\frac{(q^{1-c_0} - 1)}{(q-1)} \tag{13}$$

It can easily be shown that $\Delta c \to 0$ when $Lx \to 0$ and $Lx \to \infty$. Therefore, there exists a particular spacing Lx such that Δc is maximum. For parameter values corresponding to usual organic mixtures, this optimal spacing is of the order of 200−300 μm. In practice, experiments are conducted with spacings ranging from 1 to 2 mm, and in that case, $K_d \ll K$ (see eq 12.b), and thus, $K_t \approx K$. As a matter of fact, the ratio H/K does not depend on ΔT, the temperature difference imposed between the two vertical walls. In that case, eq 13 reduces to eq 2, which is our working equation to deduce D_T. Let us note that the separation must be experimentally independent of ΔT in order to validate eq 2. Otherwise, eq 13 should be used instead. Let us finally note that both solution 13 and its approximation 2 have been numerically recovered in 2D numerical simulation without any of the approximations mentioned above(except a Boussinesq fluid).[9]

2.3. The "Overshoot" Effect in LDV Experiments. Steady convection in a very high TGC ($A > 100$, i.e., $u = 0$) is governed by the momentum, energy and mass conservation equations

$$\nu\frac{\partial^3 w}{\partial x^3} = g\frac{\partial(\rho/\rho_0)}{\partial x} \tag{14}$$

$$w(x)\frac{\partial T}{\partial z} = \kappa\left(\frac{\partial^2 T}{\partial z^2} + \frac{\partial^2 T}{\partial x^2}\right) \tag{15}$$

$$w(x)\frac{\partial c}{\partial z} = D\left(\frac{\partial^2 c}{\partial z^2} + \frac{\partial^2 c}{\partial x^2}\right) \tag{16}$$

where w is the vertical velocity component.

The FJOM theory supposes that $(\partial T/\partial z) = 0$ (T is only a linear function of x) and that ρ is only a linear function of T. Therefore, the r.h.s. of eq 14 becomes a constant, and the integration of this equation leads to (using eq 3) with $\beta = 0$)

$$w(X) = w_0 X(X-1)\left(X-\frac{1}{2}\right);\ X = x/Lx \tag{17a}$$

$$w_0 = -g\alpha\Delta T Lx^2/6\nu \tag{17b}$$

When introduced into eq 16, with $(\partial c/\partial z) = (\Delta c/Lz) =$ constant, (given by eq 2), this leads to a polynomial of the 5th degree for $c(X)$. But it may be verified that the mean value of $c(X)$ in the rising and in the sinking liquid columns is the same

$$\int_0^{1/2} c(X)dX = \int_{1/2}^{1} c(X)dX = c_0 \tag{18}$$

and this "justifies" a posteriori the assumption that the horizontal variation of $c(X)$ does not contribute to the buoyancy force. This is not totally true because in the differential eq 14, we need "local" density gradient, not simply the difference between the "mean" right and left densities. But there is another solution to eq 16, and this is the so-called "diffusive" solution for the mass fraction field

$$\left[\begin{array}{l}\dfrac{\partial c}{\partial z} = 0\\[2ex] \dfrac{\partial c}{\partial x} = -\dfrac{D_T}{D}c_0(1-c_0)\dfrac{\Delta T}{Lx}\end{array}\right] \tag{19}$$

Clearly, the horizontal mass fraction gradient arises from the zero mass flux condition at the two vertical walls. It is clear that this "diffusive" solution for the concentration field prevails only for small time after switching on the temperature gradient. For larger time, a vertical mass fraction distribution is built up by convection, at the expense of the horizontal gradient that is almost destroyed. We introduce now eq 19 into eq 14, using the full eq 3, because in the "diffusive" regime the concentration field contributes to the buoyancy force.

Instead of eq 17a, we now have

$$w(X) = w_0(1+\psi)X(X-1)\left(X-\frac{1}{2}\right) \tag{20}$$

where ψ is the so-called separation ratio

$$\psi = \frac{\beta}{\alpha}\frac{D_T}{D}c_0(1-c_0) \tag{21}$$

and represents the concentration contribution to the horizontal density gradient, relative to the contribution coming from the temperature gradient.

In the diffusive regime, the velocity amplitude at $X = (3 \pm \sqrt{3})/6$ is

$$w_a^{\max} = w_0(1+\psi)\frac{\sqrt{3}}{36} \tag{22a}$$

whereas, in the convective regime, when the liquid layer is supposed to be horizontally "homogeneous" (this is the reason for the superscript "h")

$$w_a^{\,h} = w_0\frac{\sqrt{3}}{36} \tag{22b}$$

The value of ψ can be deduced from the two amplitudes, in the diffusive regime 22a for small time and in steady-state conditions 22b

$$\psi = \frac{w_a^{\max}}{w_a^h} - 1 \tag{23}$$

Let us summarize: when switching on the temperature gradient, the velocity amplitude, as recorded for example by LDV, starting from the zero value, reaches, a maximum value $w_a^{\max}$, after some time related to the relaxation time for diffusion and then starts to decrease to its final value w_a^h. The overshoot in the velocity amplitude is an indirect measure of S_T, through its effect on horizontal density gradient. One has to be aware of the fact that, to use eq 23, full horizontal Soret separation, given by eq 19, must be reached, and this implies that the convective regime should be delayed as long as possible. The ideal time behavior of the velocity amplitude is given by curve (a) of Figure 3. This is true if the relaxation time for diffusion $\tau_{\text{Diff}} = Lx^2/\pi^2 D$ is very small compared to the time needed for a volume element to travel from bottom to top of the TGC at velocity w_a^h (this time will be called τ_{conv})

$$\frac{Lx^2}{\pi^2 D} \ll \frac{Lz}{w_a^h} \tag{24a}$$

In dimensionless form, this inequality may be transformed into

$$\frac{\tau_{\text{conv}}}{\tau_{\text{Diff}}} = 1231\frac{A}{\text{GrSc}} \gg 1 \tag{24b}$$

where A is the aspect ratio $A = Lz/Lx$, Gr the Grashof number $\text{Gr} = g\alpha\Delta\text{T}\text{Lx}^3/\nu^2$ and Sc the Schmidt number $\text{Sc} = \nu/D$. Therefore, optimal operating conditions for observing the maximal overshoot are as follows:

- small spacing Lx
- large diffusion coefficient D
- tall cells
- small ΔT
- small α and large ν However, for a given mixture, α, ν, and D are imposed. It is also difficult to scan with the laser system and to look for the velocity amplitude if $Lx < 1.5$ mm. And technical reasons impose a maximum height of ~50 cm. Of course one could always dream of a TGC several meters high! Also, ΔT must not be too small; otherwise the velocity amplitude becomes more difficult to measure with the desired accuracy ($\Delta T = 3$ °C to 5 °C seems reasonable; we get $w_a^h =$ 118 μm/s for pure water with $Lx = 1.5$ mm and $\Delta T = 3$ °C). The cell that we have designed is only 50 cm high, and, depending on the mixture, condition 24b is not always fulfilled. In that case, the experimental velocity amplitude in the overshoot w_a^{exp} could be lower than its maximal expected value $w_a^{\max}$, and the behavior is then given by curve(b) of Figure 3. One then deduces an "effective" separation ratio ψ_e less than the real one

$$\psi_e = \frac{w_a^{\text{exp}}}{w_a^h} - 1 < \psi \tag{25}$$

and a correction factor $\gamma > 1$ has to be introduced

$$\psi = \gamma\cdot\psi_e \tag{26}$$

We explain in section 2.4 how to obtain this correction factor γ for a large range of variation of the governing parameters Sc,

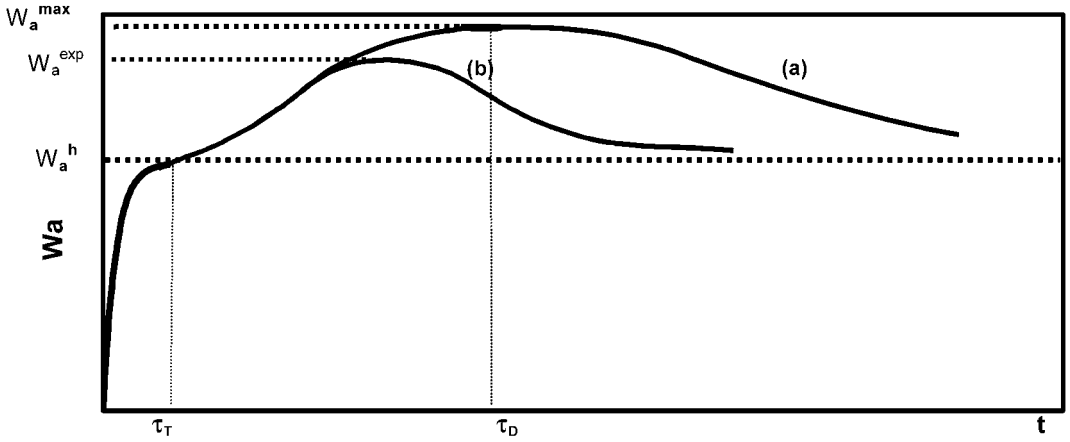

Figure 3. Temporal behavior of the velocity amplitude and the "overshoot effect" during the LDV experiments.

TABLE 1: 2D Numerical Calculations of the Correction Factor γ, Their Fitted Values, and the Obtained Differences

	1	2	3	4	5	6
parameter values	τ_{conv}/τ_{Diff}	ψ	ψ_e	γ	γ fitted	differences in %
Sc = 5000	0.821	0.1	0.0186	5.3671	5.3903	−0.4
A = 100		0.3	0.0856	3.5057	3.4596	1.3
Gr = 30		0.5	0.1470	3.3916	3.4017	−0.3
		0.8	0.2328	3.4364	3.4703	−1.0
		1.2	0.3357	3.5742	3.6076	−0.9
		1.5	0.4065	3.6903	3.7142	−0.6
Sc = 1000	1.009	0.1	0.0254	3.9374	3.9128	0.6
A = 100		0.3	0.1048	2.8636	2.8391	0.9
Gr = 122		0.5	0.1778	2.8119	2.8194	−0.3
		0.8	0.2780	2.8772	2.8924	−0.5
		1.2	0.3992	3.0059	3.0187	−0.4
		1.5	0.4825	3.1087	3.1142	−0.2
Sc = 10 000	1.231	0.1	0.0323	3.0953	3.0711	0.8
A = 150		0.3	0.1239	2.4221	2.4009	0.9
Gr = 15		0.5	0.2076	2.4081	2.3999	0.3
		0.8	0.3222	2.4830	2.4696	0.5
		1.2	0.4593	2.6127	2.5804	1.2
		1.5	0.5531	2.7118	2.6626	1.8
Sc = 1000	1.846	0.1	0.0473	2.1135	2.1148	−0.1
A = 150		0.3	0.1666	1.8008	1.8101	−0.5
Gr = 100		0.5	0.2755	1.8146	1.8237	−0.5
		0.8	0.4248	1.8832	1.8811	0.1
		1.2	0.6039	1.9871	1.9654	1.1
		1.5	0.7265	2.0648	2.0267	1.8
Sc = 2000	2.462	0.1	0.0575	1.7393	1.7516	−0.7
A = 200		0.3	0.1960	1.5310	1.5529	−1.4
Gr = 50		0.5	0.3230	1.5479	1.5667	−1.2
		0.8	0.4971	1.6092	1.6127	−0.2
		1.2	0.7063	1.6990	1.6787	1.2
		1.5	0.8500	1.7648	1.7266	2.2
Sc = 2000	3.692	0.1	0.0693	1.4433	1.4552	−0.8
A = 300		0.3	0.2322	1.2920	1.3252	−2.6
Gr = 50		0.5	0.3838	1.3026	1.3348	−2.5
		0.8	0.5939	1.3470	1.3661	−1.4
		1.2	0.8489	1.4136	1.4114	0.2
		1.5	1.0249	1.4636	1.4442	1.3
Sc = 500	4.923	0.1	0.0752	1.3295	1.3319	−0.2
A = 200		0.3	0.2524	1.1884	1.2244	−3.0
Gr = 100		0.5	0.4202	1.1898	1.2304	−3.4
		0.8	0.6564	1.2187	1.2534	−2.8
		1.2	0.9472	1.2669	1.2875	−1.6
		1.5	1.1498	1.3046	1.3125	−0.6
Sc = 1000	6.154	0.1	0.0781	1.2801	1.2674	1.0
A = 150		0.3	0.2633	1.1394	1.1691	−2.6
Gr = 30		0.5	0.4410	1.1337	1.1724	−3.4
		0.8	0.6942	1.1524	1.1898	−3.2
		1.2	1.0095	1.1887	1.2164	−2.3
		1.5	1.2305	1.2191	1.2361	−1.4

A, Gr, and ψ. But, before doing this, let us stress once again that LDV experiments give the separation ratio ψ. To deduce $S_T = D_T/D$, we need a separate evaluation (under isothermal conditions) of the two expansion coefficients α and β, eq 4a and 4b.

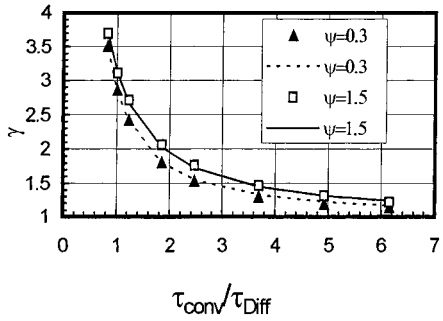

Figure 4. Evolution of the correction factor γ with the separation factor ψ and the ratio τ_{conv}/τ_{diff}.

2.4. Two-Dimensional Numerical Simulations and the Correction Factor γ. The numerical code that we have used solves the full two-dimensional Navier−Stokes, energy and mass conservation equations in time and space in the stream function-vorticity formalism. It is based on a standard finite-difference technique (21 equally spaced points along the horizontal axis and 160 grid points along the vertical axis, the spacing being smaller near the upper and lower boundaries than in the center where temperature and velocity fields are almost independent of z). The so-called ADI technique was used (see[9,20] for more numerical details). The initial conditions correspond to uniform temperature T_0, uniform mass fraction c_0 and to the rest state ($u = 0$ and $w = 0$). At time $t > 0$, the temperature difference is switched on ($T_{hot} = T_0 + \Delta T/2$ at $X = 1$; $T_{cold} = T_0 - \Delta T/2$ at $X = 0$). The upper and lower boundaries are adiabatic. The four boundaries are rigid (no slip boundary conditions; no mass flux accross these boundaries). The input parameters are the aspect ratio A, the temperature difference ΔT or, better, the Grashof number Gr, the separation ratio ψ (or $S_T = D_T/D$, together with the expansion properties of the mixture) and the Schmidt number $Sc = \nu/D$. The numerical simulation gives all the fields at each grid point and at each time step. In particular, at midheight $z = Lz/2$, the vertical velocity component $w(x,t)$ is known at each time step, thus its amplitude $w_a(t)$. The predicted time behavior of w_a, as depicted by curve(b) of Figure 3, is obtained. The maximum computed velocity amplitude, called w_a^{calc} sometimes does reach the expected value w_a^{max}, sometimes not, depending on the set of the parameters. Thus, numerically, we may define an effective separation ratio

$$\psi_e = \frac{w_a^{calc}}{w_a^h} - 1 \qquad (27)$$

The ratio between the input parameter ψ and the output

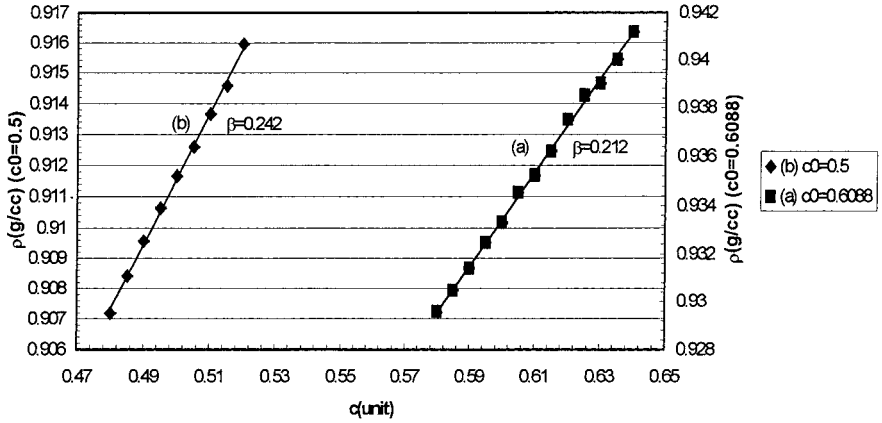

Figure 5. Evaluation of the mass expansion coefficient β for the two water−ethanol mixtures $c_0 = 0.5$ and $c_0 = 0.6088$ at $T_0 = 22.5$ °C.

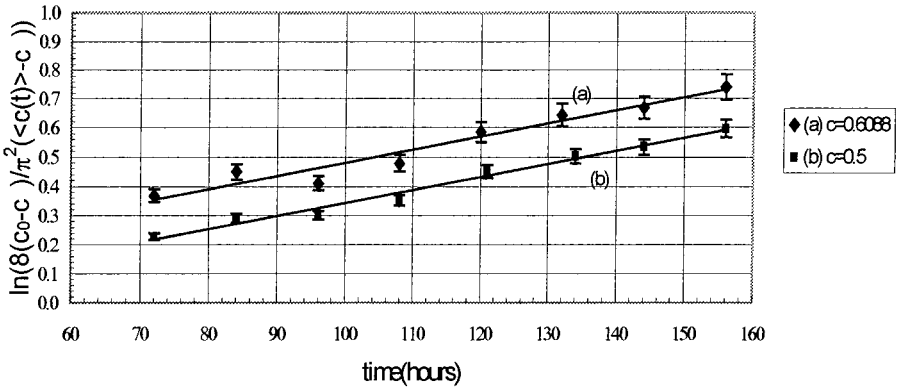

Figure 6. Diffusion curves for the experimental determination of D for the two water−ethanol mixtures $c_0 = 0.5$ and $c_0 = 0.6088$ at $T_0 = 22.5$ °C.

parameter ψ_e is the desired "correction factor" γ that takes into account the fact that pure horizontal Soret separation is not always totally achieved because the aspect ratio is finite, and sometimes the relaxation time for diffusion is too long.

The following set of parameters was used:

Sc = 500,1000, 2000, 5000, 10 000

A = 100,150, 200, 300

Gr = 15, 30, 50,100, 120

ψ = 0.1, 0.3, 0.5, 0.8, 1.2, 1.5

Results are presented in Table 1, where we give $(\tau_{conv}/\tau_{Diff})$ in column 1, according to eq 24b; in column 2, the input parameter ψ; in column 3, the output value ψ_e; and their ratio γ in column 4. Clearly, when $(\tau_{conv}/\tau_{Diff})$ increases, γ decreases and tends to 1 as depicted in Figure 4. Surprisingly, γ was also a slowly varying function of ψ. The 48 values of γ were fitted by a totally empirical law $\gamma = f((\tau_{conv}/\tau_{Diff}),\psi)$, see[21] for more details.

In col.5 of Table 1, the recalculated value of γ is given, together with the difference in col.6 with the direct 2D numerical simulation. In practice, one can say that $\gamma \approx 1$ when $(\tau_{conv}/\tau_{Diff}) > 10$.

3. Experimental Results for the Diffusion Coefficients D. Operating the OEC method, 32 tubes of internal calibrated height (29.0 ± 0.1) mm are filled with a solution $c_0 = 0.6288$ in water. The volume of each tube is ∼1 cm^3. They are placed into 4 Plexiglas holders. Four thermostated vessels (T = (22.5 ± 0.1)°C), connected to a constant-temperature bath, are filled with a solution $c_\infty = 0.5888$. The volume of the solution contained in these vessels is ∼350 cm^3. At time $t = 0$, each holder with its 8 tubes is immersed in one of the vessels which are subsenquently covered by a paraffin film pressed itself by a cork to limit the evaporation of ethanol. The solution in the tube containing more water is denser than that in the vessels. Water diffuses outside the tube and alcohol inside, until equilibrium. Each 12 h, two tubes are removed from a vessel, mixed and analyzed, by measuring the density and by comparing with a calibration curve. The timing of all previous manipulations to prepare the sample to analyze is very short (less than one minute) to avoid supplementary evaporation of ethanol. Figure 5, curve (a) shows such a calibration curve around the mean mass fraction $c = 0.6088$. In a narrow mass-fraction range, the dependence of ρ is linear. The density ρ was measured using the quartz vibrating U-tube densimeter DMA5000 manufactured by Anton PAAR. The accuracy is $\pm 2 \times 10^{-6}$ g/cm^3. From the knowledge of the mean density of the removed tubes and from the calibration curve, we have the mean mass fraction in the tubes each 12 h. Figure 6 curve (a) shows $\ln((8(c_0 - c_\infty)/\pi^2(\langle c(t)\rangle - c_\infty))$ versus time. The slope gives D/L^2; knowing L = (29.0 ± 0.1) mm, we have D. The difference of 4% in mass fraction between c_0 and c_∞ is sufficiently small to attribute the value of D to the mean value of c, i.e., to $c = (c_0 + c_\infty)/2 = 0.6088$. Finally, let us note that we have plotted the experimental points only for $t \geq 72$ h. The first points($t < 72$ h) do not fit a linear law. From the standard deviation, we estimate the accuracy on D to be of order of 5%. The error on the length L is negligible.

The procedure is repeated for $c_0 = 0.52$ and $c_\infty = 0.48$, and allows the determination of D for a mixture 0.5 mass fraction (Figure 5 curve b and Figure 6 curve b). Table 2 gives the values of D obtained in this work and a comparison with those obtained earlier by Kolodner et al.,[16] by Zhang et al.[17] and by Köhler and Müller,[19] together with the differences in parentheses.

4. Thermogravitational Experiments. *4.1. Description of the Cell (Figure 7).* The experimental cell used in this work is

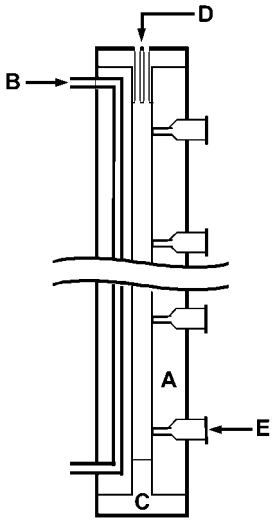

Figure 7. Sketch of the experimental TGC.

TABLE 2: Comparison between the Different Isothermal Diffusion Coefficients *D* Measured in This Work and Those Published in the Literature

system	this work $D(10^{-10}$ m^2/s)	Kolodner et al.[16] $D(10^{-10}$ m^2/s)	Zhang et al.[17] $D(10^{-10}$ m^2/s)	Kohler and Muller[19] $D(10^{-10}$ m^2/s)
$c_0 = 0.6088$	(4.32 ± 0.26)	3.82 (12%)	4.15 (4%)	4.19 (3%)
$c_0 = 0.5$	(4.2 ± 0.21)			

constructed with two vertical blocks (A) in massive copper. Inside each block, the temperature is imposed by a water flow (B) directly pumped from thermostated bath with a precision of ± 0.01 °C. The front and back faces allowing optical access in LDV experiments are realized with glass strips glued to adjacent exchangers. Brass spacers bolted at the top and the bottom of the cell (C) ensure the vertical uniformity of the fluid layer gap Lx. The upper spacer is pierced by two holes, making the air evacuation and the necessary introduction of a nozzle for the cell filling (D) easier. A lower outlet, also used for the sampling process, allows the emptying of the cell (E). The dimensions of the delimited working space are: $Lx = (1.58 \pm 0.02)$mm, $Ly = 3$ cm (cell depth), $Lz = 53$ cm ($A = 335$).

We shall come back later to the determination of *Lx*, which is a crucial problem because *Lx* appears with the power 4 in the separation Δc given by eq 2. But let us say that the spacers (C) were manufactured with a thickness exactly equal to 1.5 mm. However, they are glued in order to ensure water-tightness, and therefore, the real spacing should be a little bit greater than 1.5 mm. We dispose of a set of ceramic spacers (from Mitutoyo Company), with accuracy 0.2 μm! The spacer 1.5 mm enters everywhere in the slot; the spacer 1.6 mm does not. The most realistic value (1.58 ± 0.02 mm) of the average spacing is based, as explained in section 5.1, on velocity amplitudes recorded by LDV on 5 pure substances.

4.2. Thermogravitational Separation. Since we have 5 sampling positions, it is rather easy to determine $c(z)$, and thus the gradient Dc/Lz. Once again, each sample ($\sim$1.7 cm^3) is analyzed by densitometry. Figure 8 shows the variation of ρ with elevation in the two experiments of different initial mass fraction as discussed in the previous paragraph. The variation is quite linear. Density decreases with elevation as it should because $S_T > 0$, and therefore, the lighter component migrates to the hot plate and is advected to the top. The expansion coefficient β is deduced from the calibration curves Figure 5.

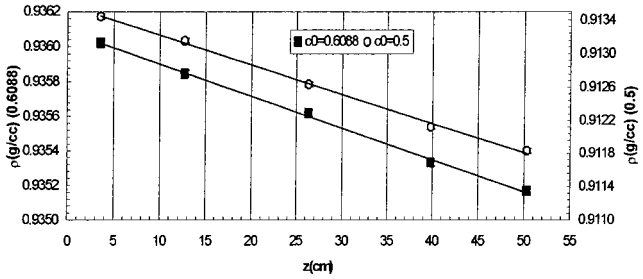

Figure 8. Experimental density profiles versus elevation *z* into the thermogravitational cell.

Next, we computethe mass fraction gradient by

$$\frac{\Delta c}{Lz} = \frac{\partial \rho / \partial z}{\rho_0 \beta} \tag{28}$$

Let us note that we begin the sampling process after $\sim$150 min, i.e., approximately five times the relaxation time of the process given by[11]

$$t_r = \frac{9! Lz^2 \nu^2 D}{(\pi \Delta T g \alpha Lx^3)^2} \tag{29}$$

and equal to $\sim$30 min for $\Delta T = 5$ °C, $Lx \approx 2$ mm and $D \approx 4 \times 10^{-10}$ m^2/s. During this short period of time, the corrosion of the brass spacers and the dissolution of the glue used for the glass strips cannot affect the quality of the results as it would be the case, e.g. in porous media where the duration of an experiment is generally several weeks. Once we have $\Delta c/Lz$ from Figure 5 giving β and Figure 8 giving $(\partial \rho / \partial z)$, using of course eq 28, we still need the thermal expansion coefficient α and the kinematic viscosity ν to compute D_T from eq 2. The thermal expansion coefficient α was deduced for each system of given mass fraction by measuring its density at different temperatures around the mean temperature of 22.5 °C, using the built-in facility of the Paar densimeter that uses a Peltier element(estimated temperature fluctuation: 0.005 °C given by the manufacturer). The densities $\rho(T)$ and α of the two systems are given in Figure 9. The kinematic viscosity was measured by a Höppler viscosimeter (falling ball). On the basis of 3 measurements, the mean values of ν are given in Table 3. The values of D_T obtained in the present work from eq 2 and the knowledge of α and ν, are given in Table 4 and are compared with those published in[18] using cylindrical columns.

5. LDV Experiments. *5.1. Case of Pure Substances.* The aim of this paragraph is to explain the filtering process, obtain the best value of *Lx*, and show the absence of any overshoot in the time evolution of the velocity amplitude, and to compare later with the behavior of a binary mixture.

In steady state conditions, the velocity profile is given by eq 17a. Experimental records of velocity profiles have been given previously,[22,23] and more graphs will not be given here even if the experimental cells that have been used in these previous papers were not specially designed to measure the separation ratio (too small aspect ratio). The main point is that, when recording steady velocity profiles along the *x* axis (an experimental point being taken usually each 100 μm sometimes each 50 μm), one may wait, at a given position, as long as we want, for example, 20 Doppler bursts, to have an average velocity at the prescribed position because there are velocity gradients in the optical probe itself (the diameter of the cross section of the measuring probe is $\sim$90 μm, not extremely small compared to the gap *Lx*). This averaging process minimizes statistical

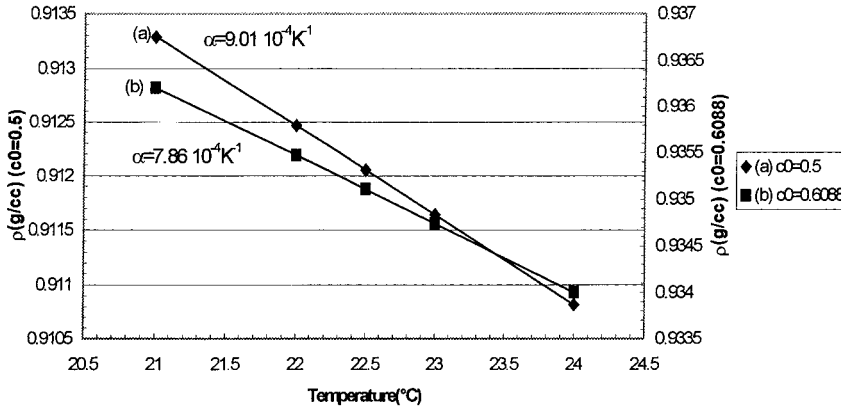

Figure 9. Evaluation of the thermal expansion coefficient α for the two water-ethanol mixtures $c_0 = 0.5$ and $c_0 = 0.6088$ at $T_0 = 22.5$ °C.

TABLE 3: Kinematic Viscosity ν of the Two Water−Ethanol Mixtures $c_0 = 0.5$ and $c_0 = 0.6088$ at $T_0 = 22.5$ °C

system	$\nu\ 10^{-6}$ m²/s
$c_0 = 0.6088$	(2.72 ± 0.01)
$c_0 = 0.5$	(2.81 ± 0.01)

TABLE 4: Comparison between the Thermal Diffusion Coefficient D_T Measured in This Work and the Value Given by Bou-Ali Et Al.[18]

system	this work $D_T(10^{-12}$ m² K⁻¹/s)	Bou-Ali et al.[18] $D_T(10^{-12}$ m² K⁻¹/s)
$c_0 = 0.6088$	(1.37 ± 0.08)	1.31
$c_0 = 0.5$	(2.49 ± 0.15)	

TABLE 5: Thermal Expansion Coefficient α, Kinematic Viscosity ν and Their Ratio α/ν for the 5 Pure Substances: Water, Tetraline, Dodecane, Ethanol, and Isobutylbenzene

	water	tetraline	dodecane	ethanol	isobutylbenzene
$\alpha(10^{-4}\,K^{-1})$	2.01	8.48	9.74	10.8	9.88
$\nu(10^{-6}m^2/s)$	0.89	2.19	1.96	1.43	1.20
$\alpha/\nu(K^{-1}s/m^2)$	226	387	497	755	823

fluctuations, and results in a velocity profile fitted by a cubic law with a small standard deviation. During the record of the steady state velocity profile, the experimental cell rests on a three-dimensional translation table, with stepping motors, 10 μm step. We are thus able to carefully catch for the maximum velocity amplitude given by eq 22b. Five pure substances were investigated: water, ethanol, dodecane, isobutylbenzene, and tetraline.

The three last chemicals were chosen because of their interest for the oil industry, and could be representative of the Soret effect in crude oil (we have an alkane: dodecane, a one-ring component: isobutylbenzene and a two-ring component: tetraline). We intend later to investigate Soret effect in mixtures of those components. Kinematic viscosity and expansion coefficient were measured at $T_0 = 22.5$ °C as explained before (Höppler viscosimeter and PAAR densitometer). Results are given in Table 5. We have plotted in Figure 10 the velocity amplitude w_a^h as a function of α/ν for these 5 substances. As it should be, according to eqs 22b and 17b, the relation is linear, and the slope is given by $(g\Delta T Lx^2\sqrt{3}/216)$. Because ΔT is known ($\Delta T = 5$ °C in the 5 experiments), we have the best estimated value of Lx: (1.60 ± 0.02) mm. Combined with the ceramic spacers observations (section 4.1), this justifies taking $Lx = 1.58$ mm as the most realistic value in TGC experiments.

A different problem is to record the time evolution of the velocity at the position X where the maximum amplitude is observed in steady conditions ($X = (3 + \sqrt{3})/6$). In that case, a time averaging process is nonsense. Nevertheless, because we expected the steady state to be reached after a few hundred seconds, we decided (using the multiple capabilities of the HP3561A Dynamic Signal Analyzer) to take the time average over 4 s. This small time interval does not allow an average over more than 5 Doppler bursts..., if they occur! Sometimes, there is only one event (one burst) during this 4 s time interval, sometimes none. Thus, the time evolution of the velocity amplitude shows large statistical fluctuations (of the order of $\pm$ 100 μm/s at the steady state), and therefore, we decided to apply a filtering technique. The Fourier transform of each Doppler burst corresponds to a given frequency (related to the velocity by multiplying this frequency by the fringe spacing, see e.g., ref 24) and has its own amplitude (related to the signal-to-noise ratio SNR). We decided to eliminate all the points for which the amplitude was smaller than 300 μV (or a SNR smaller than 3). This filtering technique results in the rejection of 70% of the recorded points. The 30% of remaining points are displayed in Figure 11 for an interval of 5000 s for $\Delta T = 5$ °C and ethanol as working fluid. In the steady state, the standard deviation is now only 35 μm/sec. The steady value is $w_a^h = (1513 \pm 35)$ μm/s, whereas the theoritical value predicted by eq 17b and 22b, using $Lx = 1.58$ mm and the physical properties of ethanol given in Table 5, is $w_a^h = 1483$ μm/s, i.e., a discrepancy of only 2%, which is highly satisfactory. But the most important feature of Figure 11 is the monotonic increase of the velocity amplitude toward its steady final value without any overshoot phenomenon.

5.2. Water-Ethanol Systems. Once again, we have investigated the two same systems as before ($c_0 = 0.6088$ and $c_0 = 0.5$). Figure 12 shows the filtered velocity amplitude up to $t = 7000$ s, under the same conditions as before ($\Delta T = 5$ °C; a time averaging over 4 s) for $c_0 = 0.5$. Clearly, the time evolution is totally different from that shown in Figure 11; there is a noticeable overshoot in the velocity amplitude that now has to be estimated. First of all, let us say that such an experiment has been repeated 4 times. The steady-state amplitude w_a^h is estimated from the experimental points taken for $t > 4500$s. In the present case, we have $w_a^h = (290 \pm 9)$ μm/s. The recorded experimental points between $t = 500$s and $t = 2500$s are fitted by a cubic law in order to estimate (by differentiation) its maximum, called $w_a^{\exp}$ (here $w_a^{\exp} = (384 \pm 7)$ μm/s). Thus, the effective separation ratio is $\psi_e = (w_a^{\exp}/w_a^h) - 1 = 0.324$. Tables 6 and 7 summarize our findings for the 4 runs performed on each system. As explained before, the effective separation ratio ψ_e has to be multiplied by a correction factor γ (see section 2.3) that takes into account the finite aspect ratio of the cell. Because we have known ν, D, α, Lx, Lz, and ΔT for each system

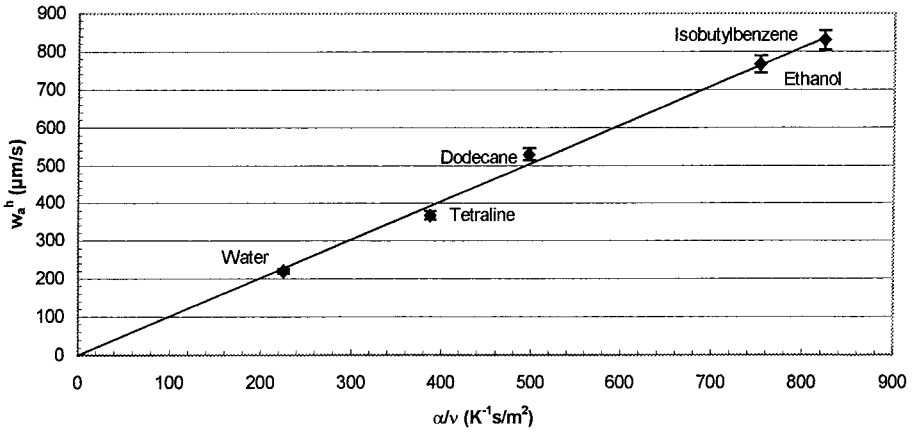

Figure 10. Steady velocity amplitude w_a^h versus ratio α/ν for 5 pure substances.

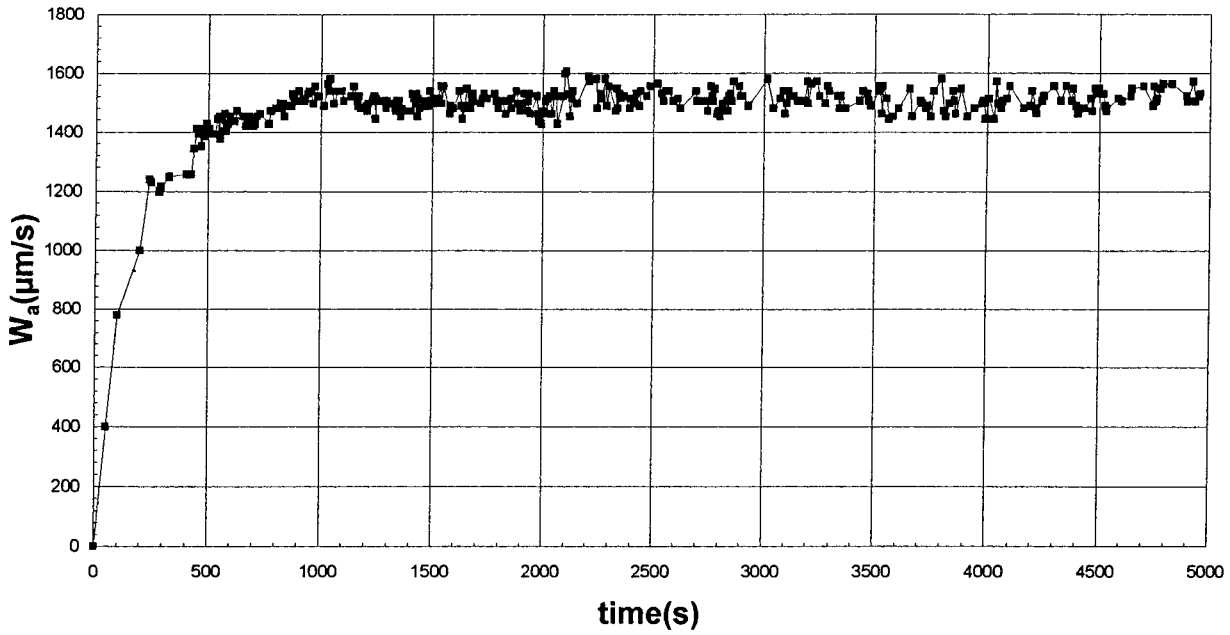

Figure 11. Temporal evolution of the velocity amplitude for pure ethanol by the LDV method.

(in other words $A = Lz/Lx$, Gr the Grashof number, and Sc the Schmidt number) we use Table 1 or Figure 4 or the empirical law to evaluate quite correctly the correction factor γ. This correction factor is given in the headings of Tables 6 and 7, together with the corrected separation ratio $\psi = \gamma\psi_e$. The standard deviation for the two systems is 7%, based on 4 runs for each system. This is quite satisfactory. Because the two expansion coefficients α and β are given on Figure 5 and Figure 9 for the two systems, we are able to evaluate the Soret coefficient $S_T = D_T/D$ (last column of Tables 6 and 7).

6. Comparison between Different Techniques, Different Laboratories and Conclusion. We have shown in section 4 that the knowledge of the vertical mass fraction distribution c(z) based on a 5-point sampling process leads finally to the determination of D_T. In section 3, a completely different experiment performed in isothermal condition, the so-called OEC technique, provides the isothermal diffusion coefficient D. We may thus compute their ratio $S_T = D_T/D$, and compare with a third completely independent experiment based on the transient enhancement of the buoyancy (or of the velocity amplitude) resulting from the Soret effect. This comparison is done in Table 8. In the last column of Table 8, we give the mean value of S_T obtained in this work, together with deviation between the two techniques in column 6. Such a small deviation between different techniques is usually not reached. Therefore, we have real confidence in our values.

It remains to compare our results with those published in the literature (see Table 9). This can be done only for one system, namely $c_0 = 0.6088$. Let us note the variety of methods used by different authors: TGC, EOC, and LDV in the present work; the deflection of a laser beam in [16,17]; thermogravitation between concentric tubes in[18] and TDFRS (Thermal Diffusion Forced Rayleigh Scattering) in.[19] Also, the mean working temperature is sometimes 25 °C[17,18] and sometimes 20 °C and 25 °C[16] (it is then easy to interpolate between these two values), whereas our mean working temperature is 22.5 °C. Anyway, the Soret coefficient, even if it is temperature dependent, should not change too much over a 2.5 °C temperature range, and thus the comparison exercise made in Table 9 is valid. The only conclusion that can be deduced from Table 9 is that the agreement is perfect and that, in contradiction to what is written in the literature,[1,2] reliable values of Soret coefficients can be obtained under terrestrial conditions, at least around room temperature for "organic" liquid mixtures. Of course, experiments could be more difficult in molten salts or liquid metals.

To end this paper, let us add some remarks concerning the application of the present techniques to negative Soret coefficients. In that case, the heaviest component is concentrated to

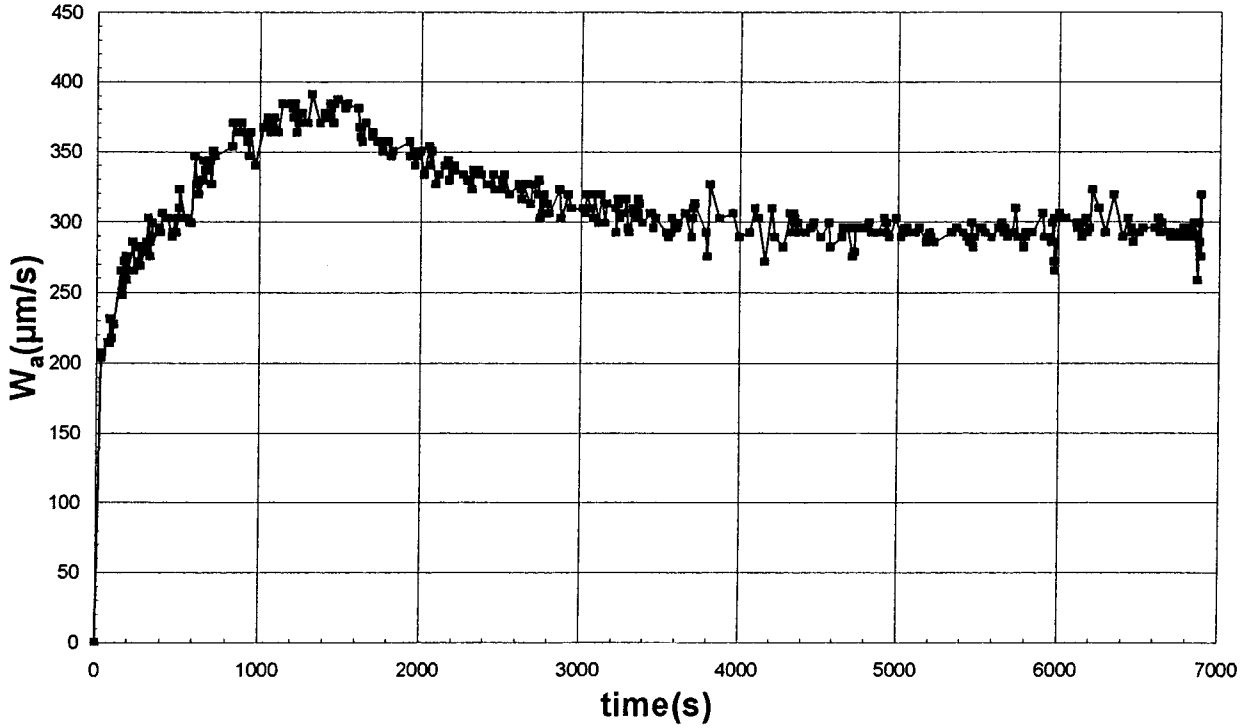

Figure 12. Temporal evolution of the velocity amplitude for the water−ethanol mixture $c_0 = 0.5$ by the LDV method.

TABLE 6: Experimental Evaluation of the Soret Coefficient by the LDV Method for the Water−Ethanol Mixture $c_0 = 0.5$ at $T_0 = 22.5$ °C

c_0=0.5, γ=1.28					
run	w_a^{exp} (μm/s)	w_a^h (μm/s)	ψ_e (10^{-1})	ψ (10^{-1})	S_T (10^{-3} K^{-1})
1	347	272	2.76	3.54	5.26
2	362	280	2.93	3.76	5.59
3	384	290	3.24	4.16	6.19
4	369	282	3.09	3.96	5.89
		mean value	3.00	3.85	5.73
		standard deviation	0.21	0.27	0.40
		standard deviation en %	7	7	7

TABLE 7: Experimental Evaluation of the Soret Coefficient by the LDV Method for the Water−Ethanol Mixture $c_0 = 0.6088$ at $T_0 = 22.5$°C

$c_0 = 0.6088$, $\gamma = 1.18$					
run	w_a^{exp} (μm/s)	w_a^h (μm/s)	ψ_e (10^{-1})	ψ (10^{-1})	S_T (10^{-3} K^{-1})
1	228	196	1.63	1.93	3.00
2	239	202	1.83	2.16	3.36
3	235	200	1.75	2.07	3.21
4	234	196	1.94	2.29	3.56
		mean value	1.79	2.11	3.28
		standard deviation	0.13	0.15	0.24
		standard deviation en %	7	7	7

the top of the thermogravitational cell and the lightest one to the bottom. This is a potentially unstable situation. Concerning this kind of behavior, a few experiments were already performed in annular TGC by Bou-Ali et al.[25] and as described in this last paper, a stable situation is only obtained when the Grashof number exceeds a critical value. Also, in our laboratory, we performed the same kind of experiments in parallelepipedic cell without obtaining a stable vertical separation in contradistinction

TABLE 8: Summary of the Soret Coefficients Values Obtained in This Work by the Two Different Methods and for the Water−Ethanol Mixtures $c_0 = 0.5$ and $c_0 = 0.6088$ at $T_0 = 22.5$ °C

1	2	3	4	5	6	7
c_0	D_T(10^{-12} m^2 K^{-1}/s) from TGC	D(10^{-10} m^2/s) from OEC	S_T (10^{-3} K^{-1}) = col2/col3	S_T (10^{-3} K^{-1}) from LDV	deviation %	$\langle S_T \rangle$ (10^{-3} K^{-1}) mean value
0.6088	1.37	4.32	3.17	3.28	3.4	3.23
0.5	2.49	4.20	5.93	5.70	4	5.82

TABLE 9: Recapitulative Comparison of the Soret Coefficients Values Measured in This Work and Published in the Literature for the Water−Ethanol Mixture $c_0 = 0.6088$ at $T_0 = 22.5$ °C

	S_T (10^{-3} K^{-1})				
c_0	this work[a]	Kolodner et al.[c]	Zhang et al.[b]	Bou-Ali et al.[b,d]	Koehler and Muller[b]
0.6088		[16]	[17]	[18]	[19]
	3.23	3.32	3.21	3.22	3.25

[a] 22.5 °C. [b] 25 °C. [c] Interpolated at 22.5 °C between values given at 20 °C and 25 °C. [d] [18], the thermal diffusion factor α is related to the Soret coefficient by $S_T = \alpha/T_0$ ($T_0 = 298.15$ K).

with annular TGC. These facts can only be explained by a hydrodynamic stability analysis, left for a future work. However, for negative S_T, it has been known for a long time that the measurement of the critical Rayleigh number in a Bénard configuration, together with the Hopf frequency is totally adapted for precise measurements of negative S_T.[26,27] In conclusion, whatever the sign of S_T, there is always a technique suitable for its correct determination under terrestrial conditions.

Acknowledgment. The authors are gratefull to the FNRS, Brussels, for supporting the research.

References and Notes

(1) Firoozabadi, A.; Ghorayeb, K.; Shukla, K. *AIChE J.* **2000**, *46*(5), 892.

(2) Van Vaerenbergh, S.; Legros, J. C. *J. Phys. Chem. B* **1998**, *102*, 4426.
(3) Clusius, K.; Dickel, G. *Naturwissenschaften* **1939**, *27*, 148.
(4) Montel, F. *Entropie* **1994**, *184/185*, 86.
(5) Furry, W. H.; Jones, R. C.; Onsager, L. *Phys. Rev.* **1939**, *55*, 1083.
(6) Jones, R. C.; Furry, W. H. *Rev. Mod. Phys.* **1946**, *18*(2), 151.
(7) Majumdar, S. D. *Phys. Rev.* **1951**, *81*(5), 844.
(8) De Groot, S. R. PhD Thesis, Noord-Hollandsche Uitgevers, 1945.
(9) Chavepeyer, G.; Platten, J. K. *Entropie* **1996**, *198/199*, 25.
(10) Ecenarro, O.; Madariaga, J. A.; Navarro, J.; Santamaria, C. M.; Carrion, J. A.; Saviron, J. M. *Macromelecules* **1994**, *27*, 4968.
(11) Bou-Ali, M. M.; Ecenarro, O.; Madariaga, J. A.; Santamaria, C. M.; Valencia, J. J. *J. Phys.: Condenser. Matter* **1998**, *10*, 3321.
(12) Bou-Ali, M. M.; Ecenarro, O.; Madariaga, J. A.; Santamaria, C. M.; Valencia, J. *J. Non-Equilib. Thermodyn.* **1999**, *24*, 228.
(13) Prigogine, I.; De Brouckère, L.; Amand, R. *Physica* **1950**, *16*, 577.
(14) Ecenarro, O.; Madariaga, J. A.; Navarro, J.; Santamaria, C. M.; Carrion J. A.; Saviron, J. M. *J. Phys. Condenser. Matter* **1990**, *2*, 2289.
(15) Wakeham, W. A.; Nagashima, A.; Sengers, J. V. *Measurement of the Transport Properties of Fluids, Experimental Thermodynamics Vol. III*; Blackwell Scientific Publications: Oxford, London, Edinburgh, Boston, Melbourne, Paris, Berlin, Vienna, 1991; Chapter 9.
(16) Kolodner, P.; Williams, H.; Moe, C. J. *Chem. Phys*. **1988**, *88*(10), 6512.
(17) Zhang, K. J.; Briggs, M. E.; Gammon, R. W.; Sengers, J. V. *J. Chem. Phys.* **1996**, *104*(17), 6881.
(18) Bou-Ali, M. M.; Ecenarro, O.; Madariaga, J. A.; Santamaria C. M.; Valencia, J. J. *Entropie* **1999**, *218/219*, 5.
(19) Köhler, W.; Müller, J. *Chem. Phys.* **1995**, *103*(10), 4367.
(20) Chavepeyer, G. PhD Thesis, Univerité de Mons, 1974.
(21) Dutrieux, J. F. PhD Thesis, Université de Mons, 2002.
(22) Chavepeyer, G.; Platten, J. K. *Entropie* **1996**, *198/199*, 10.
(23) Chavepeyer, G.; Platten, J. K.; Bada, M. B. *Appl. Sci. Res.* **1995**, *55*, 1.
(24) Platten, J. K.; Villers, D.; Villers, O. *Laser Anemometry in Fluid Mechanics-III*, Ladoan-Instituto Superior Technico-Lisbon-Portugal, 245, 1986.
(25) Bou-Ali, M. M.; Ecenarro, O.; Madariaga, J. A.; Santamaria, C. M. *Phys. Rev. E* **1999**, *59*(1), 1250.
(26) Kolodner, P.; Passner, A.; Surko, C. M.; Walden, R. W. *Phys. Rev. Lett.* **1986**, *56*, 2621.
(27) For a review, see: Platten, J. K.; Dutrieux, J. F.; Chavepeyer, G. *Proceedings of IMT4*, Bayreuth, Lectures Notes in Physics, to appear 2002.